

# Increased future ice discharge from Antarctica owing to higher snowfall

R. Winkelmann<sup>1,2</sup>, A. Levermann<sup>1,2</sup>, M. A. Martin<sup>1,2</sup> & K. Frieler<sup>1</sup>

Anthropogenic climate change is likely to cause continuing global sea level rise<sup>1</sup>, but some processes within the Earth system may mitigate the magnitude of the projected effect. Regional and global climate models simulate enhanced snowfall over Antarctica, which would provide a direct offset of the future contribution to global sea level rise from cryospheric mass loss<sup>2,3</sup> and ocean expansion<sup>4</sup>. Uncertainties exist in modelled snowfall<sup>5</sup>, but even larger uncertainties exist in the potential changes of dynamic ice discharge from Antarctica<sup>1,6</sup> and thus in the ultimate fate of the precipitation-deposited ice mass. Here we show that snowfall and discharge are not independent, but that future ice discharge will increase by up to three times as a result of additional snowfall under global warming. Our results, based on an ice-sheet model<sup>7</sup> forced by climate simulations through to the end of 2500 (ref. 8), show that the enhanced discharge effect exceeds the effect of surface warming as well as that of basal ice-shelf melting, and is due to the difference in surface elevation change caused by snowfall on grounded versus floating ice. Although different underlying forcings drive ice loss from basal melting versus increased snowfall, similar ice dynamical processes are nonetheless at work in both; therefore results are relatively independent of the specific representation of the transition zone. In an ensemble of simulations designed to capture ice-physics uncertainty, the additional dynamic ice loss along the coastline compensates between 30 and 65 per cent of the ice gain due to enhanced snowfall over the entire continent. This results in a dynamic ice loss of up to 1.25 metres in the year 2500 for the strongest warming scenario. The reported effect thus strongly counters a potential negative contribution to global sea level by the Antarctic Ice Sheet.

During the past decade, the Antarctic Ice Sheet has lost volume at a rate comparable to that of Greenland<sup>6</sup>. The enhanced moisture-carrying capacity of a warming atmosphere, on the other hand, strongly suggests increasing snowfall over Antarctica, as projected by global<sup>9</sup> and regional climate models<sup>5</sup>. This may lead to a net negative contribution of Antarctica to future sea level, depending on the magnitude of dynamic effects possibly compensating or even overcompensating this ice gain. Because surface melt will remain small even under strong climate change<sup>2,3</sup>, the major uncertainty in sea-level projections from Antarctica arises from the unknown dynamic contribution. The main mechanisms for dynamic ice loss in future climate scenarios discussed so far are softening of the ice due to surface warming<sup>10</sup>, acceleration of ice streams through the reduction or loss of an adjacent ice-shelf<sup>11</sup> and an increase in driving stress at the grounding line due to enhanced basal melting at the underside of the shelves caused by a rise in ocean temperature<sup>12</sup>, all potentially resulting in higher ice flux across the grounding line (separating the grounded ice sheet from the floating ice shelves) (Fig. 1).

In a perturbed ice-physics ensemble, we estimate a significant additional effect of dynamic ice discharge, which is caused by the projected increase in snowfall itself. As detailed below, this effect makes the largest contribution to future ice loss, as projected by the continental-scale Potsdam Parallel Ice-Sheet Model (PISM-PIK)<sup>7</sup> with a

consistent representation of the flow in the ice sheet, ice shelves and the transition zone relevant for the fast dynamics<sup>13</sup>. The underlying mechanism is simple and very robust, and consequently the effect is found along almost the entire coastline of Antarctica (Supplementary Fig. 1). It is due to a steepening of the surface gradient near the grounding line and the associated increase in the driving stress acting on the ice flow: additional snowfall increases the surface elevation of grounded ice as well as that of the floating ice shelf. Owing to the floating the resulting change in surface elevation is, however, ten times larger on grounded ice than on the floating shelf for the same amount

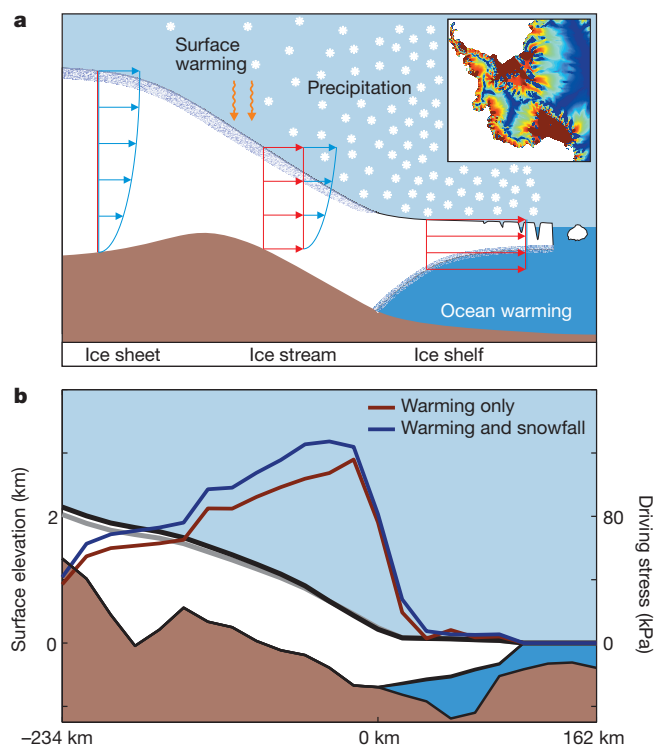


**Figure 1 | Main mechanisms of dynamic ice loss.** **a**, Conceptual figure illustrating the various forcings acting on the ice sheet. Inset, velocity field of a present-day Antarctic Ice Sheet simulation with PISM-PIK, which models the different flow regimes in sheet, streams and shelves in a consistent manner. The approach allows for the transition from vertical-shearing dominated flow of grounded ice to spreading-dominated flow in ice shelves. The resulting range in ice velocity spans several orders of magnitude and compares well with observational data<sup>27</sup>. Velocity profiles are illustrated as blue lines for the vertical-shearing-dominated and red lines for the spreading-dominated flow. **b**, Ice contours for the years 2000 (light grey) and 2500 (black) of the ECP 8.5 scenario with enhanced snowfall (for the section depicted in Supplementary Fig. 1b). Enhanced snowfall leads to an increase in surface elevation on the sheet, whereas the elevation of the ice shelf remains almost constant because it floats. The corresponding driving stress with snowfall change (blue) is significantly higher than for the simulation with warming only (red).

<sup>1</sup>Potsdam Institute for Climate Impact Research (PIK), 14473 Potsdam, Germany. <sup>2</sup>Physics Institute, Potsdam University, 14476 Potsdam, Germany.

of accumulated snow. In the simulations, this increase in surface gradient can be observed in all coastal regions of the Antarctic Ice Sheet; it is also observed when the initial states are forced by snowfall changes projected by regional climate models. It yields an increase in driving stress and hence ice transport across the grounding line (as shown for an exemplary profile of the coastal region of the Amundsen Sea sector in Fig. 1b). As a rule of thumb, the effect is larger than the increase in driving stress induced by enhanced sub-shelf melting as long as the rate of basal melt is less than nine times the snowfall, which is generally the case in all projections presented here (Fig. 2). Under very strong climatic forcing a few regions, such as the catchment area of the Ross Ice Shelf, show a retreat of the grounding line. Here additional snowfall may lead to an increase in the buttressing ability of the ice shelf, countering the effects of enhanced sub-shelf melting and limiting the acceleration of ice flux upstream of the grounding line. In all other regions and under less extreme climatic forcing, snowfall enhances ice loss.

Although projections of Antarctic temperature and snowfall changes are subject to substantial uncertainty<sup>9</sup>, a robust feature of both global and regional model simulations that is relevant for the dynamic effect presented here is the increase in snowfall along the coastal margins<sup>5</sup>. The climate scenarios applied here are based on the Representative Concentration Pathways (RCPs), which span the full range of radiative forcing from 2.6 to 8.5 W m<sup>-2</sup> projected up until the end of the twenty-first century; after this, we used the respective Extended Concentration Pathways (ECPs)<sup>14</sup> until 2500. Using a statistical downscaling method<sup>8</sup>, the corresponding global-mean temperature changes (as obtained from emulations of the full range of CMIP3 atmosphere–ocean general circulation model (AOGCM) responses<sup>15</sup> using MAGICC 6.0<sup>16</sup>) were transferred into scenarios for the surface temperature over Antarctica and the ocean temperature near the major ice shelves. The basal-melt rate underneath each of the shelves was computed from the shelf's geometry and the temperature and salinity at its cavity entrance, using a simplified ocean model for the circulation in sub-ice-shelf cavities<sup>17</sup>.

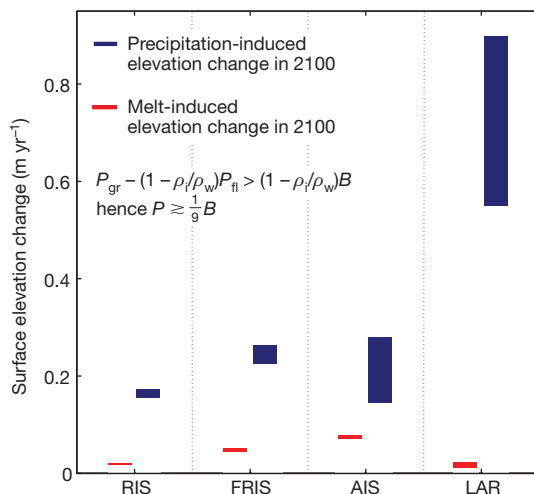


**Figure 2 | Comparison of drivers of dynamic ice loss.** Given is the model spread (for the perturbed-physics ensemble) of the surface elevation changes at the grounding lines of the Ross (RIS), Filchner-Ronne (FRIS), Amery (AIS) and Larsen (LAR) Ice Shelves in the year 2100 compared to pre-industrial values. Whereas enhanced basal melting induces a surface elevation change of  $[1 - (\rho_i/\rho_w)]B$  at the grounding line (shown in red), the surface elevation change due to snowfall (shown in blue) is given by  $P_{gr} - [1 - (\rho_i/\rho_w)]P_{\eta}$ , where  $\rho_i$  and  $\rho_w$  are the density of ice and ocean water, respectively,  $B$  is the sub-shelf melt rate at the grounding line and  $P_{gr}$  and  $P_{\eta}$  denote the snowfall rate upstream and downstream of the grounding line, respectively. Both the sub-shelf melt rate  $B$  and the snowfall rate  $P$  are given in metres per year. Snowfall-driven ice loss will thus dominate basal-melt driven ice loss if the snowfall rate at the grounding line is larger than approximately one-ninth of the basal melt rate at the grounding line.

Recently observed values for the Ross<sup>18</sup>, Filchner<sup>19</sup>–Ronne<sup>20</sup> and Amery<sup>21</sup> Ice Shelves as well as the shelf attached to Pine Island Glacier<sup>22</sup> are captured by the modelled range for the year 2000. Precipitation changes are parameterized following ref. 23 and account for temperature increase as well as for changes in ice topography. As detailed elsewhere<sup>24</sup>, we seek to capture the uncertainty that arises from different global climate sensitivity as well as the uncertainty due to ice-model parameters. To this end, each ECP scenario is represented by the median and the upper and lower 33rd percentile of the uncertainty distribution for the Antarctic temperature pathways originating from the inter-AOGCM variations and the uncertainty of the global mean temperature change from MAGICC 6.0. Furthermore, each of these  $4 \times 3$  (scenarios  $\times$  percentiles) simulations was carried out starting from an ensemble of 81 initial states with different ice-parameter settings. All of these initial states closely resemble present-day Antarctica in ice volume and geometry, but differ in ice softness and the friction between ice sheet and

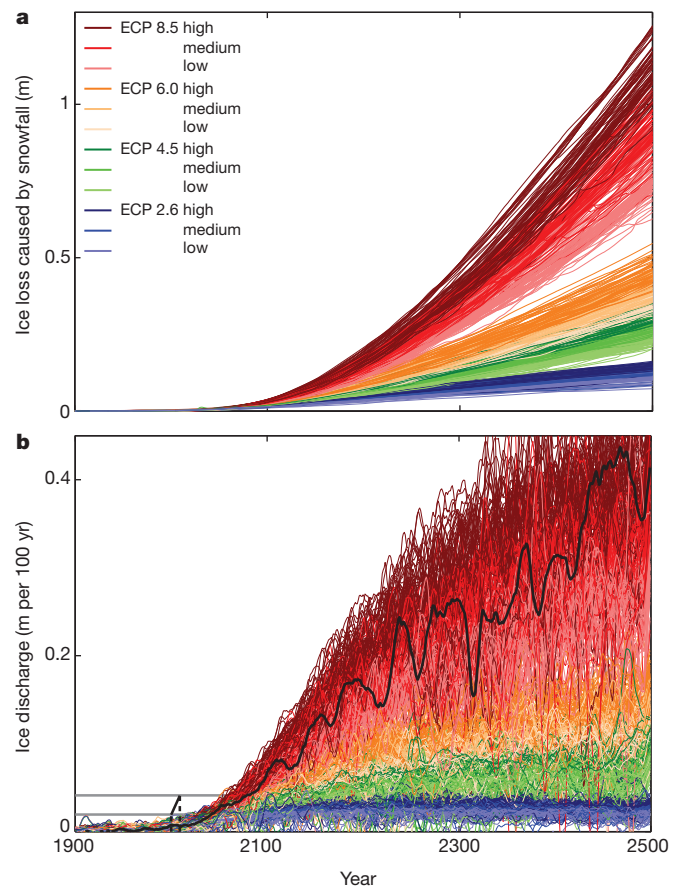


**Figure 3 | Time series of snowfall-induced ice loss.** **a**, Difference in solid ice loss between full scenario simulations and simulations with warming only, given in metres of sea-level equivalent. The additional ice loss due to enhanced snowfall increases for all scenarios with time. The spread from unknown physics captured in the 81-member ensemble is smaller than the range spanned by the medians for each scenario. **b**, Associated additional solid ice discharge, given in metres of sea-level equivalent per century. The model is in principle capable of reproducing the currently observed solid ice discharge from Antarctica (horizontal grey lines)<sup>6</sup> of 0.2–0.4 mm yr<sup>-1</sup> for the years 2000 to 2009 and the associated acceleration within this time-period (thick black line; dashed lines indicate  $x$ -intercepts). These values are, however, reached later within the twenty-first century. As an example, the additional solid ice discharge is marked for one specific ensemble member by a thin black line, illustrating that the currently observed acceleration is within the variability of the additional ice discharge projected for ECP 8.5. The present study does not rely on the exact projection of ice loss from Antarctica but reports the relative importance of enhanced snowfall for the increase in future ice discharge compared to surface and ocean warming.

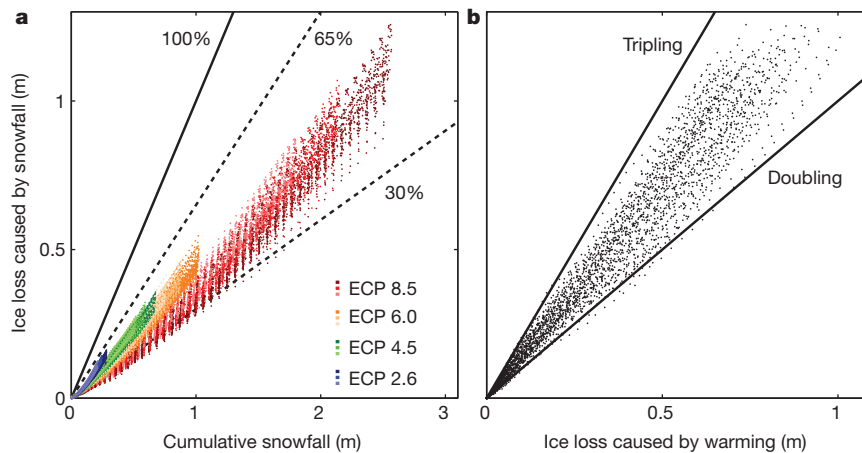


**Figure 4 | Snowfall-induced ice loss compared to ice gain from precipitation and ice loss from warming only.** All values are given in metres of sea-level equivalent. **a**, The additional ice loss under the ECP scenarios correlates with the cumulative amount of additional snowfall during the simulations. It compensates between 30% and 65% (shown as dashed black lines) of the ice gain due to enhanced snowfall. The percentage depends on the climate scenario—it is highest for the weak ECP 2.6 and lowest for the strong ECP 8.5.

basal topography and therefore in their sensitivity to a change in the climatic boundary conditions. For details of the model and ensemble simulations, see Methods section and ref. 24.

To estimate the influence of snowfall on ice discharge, we conducted simulations with surface and oceanic warming only as well as simulations with additional snowfall using the entire 81-member ensemble. Whereas the median of warming-induced ice loss in the year 2500 ranges from 0.04 m sea-level equivalent for the ECP 2.6 scenario to 0.65 m for the ECP 8.5 scenario, additional snowfall leads to a negative total mass balance in the range from  $-0.08$  m for the ECP 2.6 scenario to  $-0.56$  m sea-level equivalent for the ECP 8.5 scenario. These estimates of future mass loss are likely to be conservative for several reasons: additional mass loss might be caused by dynamic effects such as the marine ice sheet instability as well as the reduction of buttressing due to the retreat or collapse of surrounding ice shelves. It is also noteworthy that the projected snowfall increases represent a best-case scenario for mitigating Antarctica's contribution to sea level rise under continued oceanic and atmospheric warming. In contrast, if snowfall trends remain insignificant, as they have during the past decades<sup>25</sup>, the sea level contribution of the Antarctic Ice Sheet will be even larger.

The amount of ice flowing across the grounding line in excess of the flux balancing the enhanced snowfall is called dynamic ice loss. For the entire ensemble, the difference in dynamic ice loss between the full scenarios and those with warming only—that is, the snowfall-induced ice discharge—increases throughout the simulations, amounting to 0.07–0.16 m sea-level equivalent for the ECP 2.6 scenario, and 0.63–1.25 m sea-level equivalent for the ECP 8.5 scenario with ensemble means of 0.12 m and 0.92 m, respectively, in the year 2500 (Fig. 3a). PISM-PIK is in principle capable of reproducing a dynamic situation where the ice discharge is of the magnitude and rate currently observed in satellite data<sup>6</sup>, though much later in this century (Fig. 3b). This may be because all scenarios start from an ensemble of equilibrium simulations that may not be the appropriate initialization for a future projection. The results presented here do not rely on this initialization, however; they report the relative importance of snowfall compared to other currently discussed ice-loss processes.

The snowfall-induced ice discharge correlates strongly with the cumulative amount of snowfall, compensating between 30% and 65% of the additional ice volume from the projected increase in precipitation (Fig. 4a). The ratio of this snowfall-induced ice discharge over cumulative snowfall changes predominantly with the warming

For each scenario, the model was forced with the median as well as the upper and lower borders of the likely range of warming: that is, the 50th, the 66th and the 33rd percentile of the spread generated by climate projections. **b**, Dynamic ice loss through snowfall exceeds ice loss through warming. The ice loss from both snowfall and warming amounts to 200% to 300% of the ice loss through warming only.

scenario, ranging, in the year 2500, from 35–50% for the high-emission scenario ECP 8.5, to 48–60% for the weaker ECP 2.6, in which global mean temperature is kept below two degrees with respect to pre-industrial levels<sup>14</sup>. The effect is thus highest for low warming scenarios, which might be due to the time-delay of the ice-sheet response to atmospheric forcing. The ice loss caused by the additional snowfall is larger than the ice loss from the combined warming of ice surface and the ocean. It amounts to 100%–200% of the volume change found in the warming-only simulations (Fig. 4b). Here the change in ice softness due to surface warming results in higher ice loss than the warming-induced basal melting, but both effects are significantly smaller than the ice loss caused by additional snowfall (Supplementary Fig. 2).

Our study thus shows that an increase in snowfall over Antarctica under global warming results in additional dynamic ice loss. For future climate scenarios based on the ECPs, this contribution is significantly larger than the dynamic ice loss due to warming only. This is consistent with the fact that the regional rate of snowfall increases the surface gradient across the grounding line nine times stronger than the equivalent rate of basal melt.

## METHODS SUMMARY

Simulations were carried out with the Potsdam Parallel Ice Sheet Model, PISM-PIK, as described in ref. 7, extended by an ocean box model<sup>17</sup> that simulates the main overturning circulation in sub-ice shelf cavities. Lack of knowledge about the values of the model input parameters introduces an uncertainty into the projections of future ice discharge. To capture this uncertainty, we perturbed the parameters that are most relevant for the ice flow across the grounding line. These are the two so-called enhancement factors (which determine the ice viscosity in the ice sheet, ice streams and ice shelves) and the pore-water fraction (which influences basal friction). For each parameter configuration, an equilibrium state of the Antarctic Ice Sheet under present-day boundary conditions<sup>26</sup> was generated via the spin-up procedure described in ref. 27. We then excluded those initial states whose geometry deviates strongly from present-day observations. In particular, both the sea-level relevant volume of the West Antarctic Ice Sheet and the grounding line position may not differ by more than 10% from their observed values. The remaining 81 representations of the Antarctic Ice Sheet, which span the widest possible range of dynamic sensitivity compatible with these criteria, served as initial states for the simulations discussed here. They were forced by surface and ocean temperature trajectories based on the ECPs that were derived via a statistical downscaling method<sup>8</sup> from the corresponding global-mean-temperature changes. The dynamic response of the perturbed-physics ensemble to the ECP scenarios is further discussed in ref. 24.



**Full Methods** and any associated references are available in the online version of the paper.

**Received 16 February; accepted 27 September 2012.**

- Meehl, G. *et al.* in *Climate Change 2007: The Physical Science Basis* (eds Solomon, S. *et al.*) 747–845 (Cambridge Univ. Press, 2007).
- Huybrechts, P. *et al.* Response of the Greenland and Antarctic ice sheets to multi-millennial greenhouse warming in the Earth system model of intermediate complexity LOVECLIM. *Surv. Geophys.* **32**, 397–416 (2011).
- Vizcaíno, M., Mikolajewicz, U., Jungclauss, J. & Schurgers, G. Climate modification by future ice sheet changes and consequences for ice sheet mass balance. *Clim. Dyn.* **34**, 301–324 (2010).
- Schewe, J., Levermann, A. & Meinshausen, M. Climate change under a scenario near 1.5 °C of global warming: monsoon intensification, ocean warming and steric sea level rise. *Earth Syst. Dyn.* **2**, 25–35 (2011).
- Krinner, G., Magand, O., Simmonds, I., Genthon, C. & Dufresne, J. Simulated Antarctic precipitation and surface mass balance at the end of the twentieth and twenty-first centuries. *Clim. Dyn.* **28**, 215–230 (2007).
- Rignot, E., Velicogna, I., van den Broeke, M. R., Monaghan, A. & Lenaerts, J. Acceleration of the contribution of the Greenland and Antarctic ice sheets to sea level rise. *Geophys. Res. Lett.* **38**, L05503, <http://dx.doi.org/10.1029/2011GL046583> (2011).
- Winkelmann, R. *et al.* The Potsdam Parallel Ice Sheet Model (PISM-PIK). Part 1: Model description. *Cryosphere* **5**, 715–726 (2011).
- Frieler, K., Meinshausen, M., Mengel, M., Braun, N. & Hare, W. A scaling approach to probabilistic assessment of regional climate change. *J. Clim.* **25**, 3117–3144 (2012).
- Uotila, P., Lynch, A. H., Cassano, J. J. & Cullather, R. I. Changes in Antarctic net precipitation in the 21st century based on Intergovernmental Panel on Climate Change (IPCC) model scenarios. *J. Geophys. Res.* **112**, D10107, <http://dx.doi.org/10.1029/2006JD007482> (2007).
- Larour, E., Rignot, E., Joughin, I. & Aubrey, D. Rheology of the Ronne Ice Shelf, Antarctica, inferred from satellite radar interferometry data using an inverse control method. *Geophys. Res. Lett.* **32**, L05503, <http://dx.doi.org/10.1029/2004GL021693> (2005).
- Dupont, T. K. & Alley, R. B. Assessment of the importance of ice-shelf buttressing to ice-sheet flow. *Geophys. Res. Lett.* **32**, L04503, <http://dx.doi.org/10.1029/2004GL020204> (2005).
- Rignot, E. & Jacobs, S. S. Rapid bottom melting widespread near Antarctic ice sheet grounding lines. *Science* **296**, 2020–2023 (2002).
- Schoof, C. & Hindmarsh, R. C. A. Thin-film flows with wall slip: an asymptotic analysis of higher order glacier flow models. *Q. J. Mech. Appl. Math.* **63**, 73–114 (2010).
- Meinshausen, M. *et al.* The RCP greenhouse gas concentrations and their extensions from 1765 to 2300. *Clim. Change* **109**, 213–241 (2011).
- Meehl, G. A. *et al.* THE WCRP CMIP3 multimodel dataset: a new era in climate change research. *Bull. Am. Meteorol. Soc.* **88**, 1383–1394 (2007).
- Meinshausen, M., Raper, S. C. B. & Wigley, T. M. L. Emulating IPCC AR4 atmosphere-ocean and carbon cycle models for projecting global-mean, hemispheric and land/ocean temperatures: MAGICC 6.0. *Atmos. Chem. Phys. Discuss.* **8**, 6153–6272 (2008).
- Olbers, D. & Hellmer, H. A box model of circulation and melting in ice shelf caverns. *Ocean Dyn.* **60**, 141–153 (2010).
- Dinniman, M. S., Klinck, J. M. & Smith, W. O. Influence of sea ice cover and icebergs on circulation and water mass formation in a numerical circulation model of the Ross Sea, Antarctica. *J. Geophys. Res.* **112**, C11013, <http://dx.doi.org/10.1029/2006JC004036> (2007).
- Grosfeld, K. *et al.* in *Ocean, Ice and Atmosphere: Interactions at Antarctic Continental Margin* (eds Jacobs, S. S. & Weiss, R.) 83–100 (AGU Antarctic Research Ser. Vol. 75, American Geophysical Union, 1998).
- Joughin, I. & Padman, L. Melting and freezing beneath Filchner-Ronne Ice Shelf, Antarctica. *Geophys. Res. Lett.* **30**, 1477, <http://dx.doi.org/10.1029/2003GL016941> (2003).
- Williams, M. J. M., Grosfeld, K., Warner, R. C., Gerdes, R. & Determann, J. Ocean circulation and ice-ocean interaction beneath the Amery Ice Shelf, Antarctica. *J. Geophys. Res.* **106**, 22383–22400 (2001).
- Payne, A. J. *et al.* Numerical modeling of ocean-ice interactions under Pine Island Bay's ice shelf. *J. Geophys. Res.* **112**, C10019, <http://dx.doi.org/10.1029/2006JC003733> (2007).
- Huybrechts, P. & Wolde, J. D. The dynamic response of the Greenland and Antarctic ice sheets to multiple-century climatic warming. *J. Clim.* **12**, 2169–2188 (1999).
- Winkelmann, R., Levermann, A., Frieler, K. & Martin, M. A. Uncertainty in future solid ice discharge from Antarctica. *Cryosphere Discuss.* **6**, 673–714 (2012).
- Monaghan, A. J. *et al.* Insignificant change in Antarctic snowfall since the International Geophysical Year. *Science* **313**, 827–831 (2006).
- Le Brocq, A. M., Payne, A. J. & Vieli, A. An improved Antarctic dataset for high resolution numerical ice sheet models (ALBMAP v1). *Earth Syst. Sci. Data* **2**, 247–260 (2010).
- Martin, M. A. *et al.* The Potsdam Parallel Ice Sheet Model (PISM-PIK). Part 2: Dynamic equilibrium simulation of the Antarctic Ice Sheet. *Cryosphere* **5**, 727–740 (2011).

**Supplementary Information** is available in the online version of the paper.

**Acknowledgements** This study was supported by the German Federal Ministry of Education and Research (BMBF, grant 01LP1171A) and the German Federal Ministry for the Environment, Nature Conservation and Nuclear Safety (BMU, grant 11\_IL\_093\_Global\_A\_SIDS and LDCs).

**Author Contributions** R.W. and A.L. designed and performed the research. M.A.M. contributed to the discussion of the results. K.F. provided the climate forcing. R.W. wrote the paper.

**Author Information** Reprints and permissions information is available at [www.nature.com/reprints](http://www.nature.com/reprints). The authors declare no competing financial interests. Readers are welcome to comment on the online version of the paper. Correspondence and requests for materials should be addressed to R.W. ([ricarda.winkelmann@pik-potsdam.de](mailto:ricarda.winkelmann@pik-potsdam.de)).



## METHODS

**Perturbed-physics ensemble.** Simulations were carried out with the Potsdam Parallel Ice Sheet Model, PISM-PIK, as described in ref. 7. Lack of knowledge about the values of the model input parameters introduces an uncertainty into the projections of future ice discharge. To capture this uncertainty, we perturbed the parameters that are most relevant for the ice flow across the grounding line. These are the two so-called enhancement factors (which determine the ice viscosity in the ice sheet, ice streams and ice shelves) and the pore-water fraction (which influences basal friction). For each parameter configuration, an equilibrium state of the Antarctic Ice Sheet under present-day boundary conditions<sup>26</sup> was generated via the spin-up procedure described in ref. 27. We then excluded those initial states whose geometry deviates strongly from present-day observations. In particular, both the sea-level relevant volume of the West Antarctic Ice Sheet and the grounding-line position may not differ by more than 10% from their observed values. The remaining 81 representations of the Antarctic Ice Sheet, which span the widest possible range of dynamic sensitivity compatible with these criteria, served as initial states for the simulations discussed here.

**Climate scenarios.** The climate scenarios for our simulations are based on the ECPs<sup>14</sup>, which are the extensions of the RCPs<sup>28,29</sup>. Global mean temperature trajectories were obtained from emulations of the full range of CMIP3 AOGCM responses<sup>15</sup> using MAGICC 6.0<sup>16</sup>. The global mean temperature shows a close linear relation to the surface temperature over Antarctica as well as the ocean temperature near the major Antarctic ice shelves. Using the method described in ref. 8, the scaling coefficients were derived and then used to compute the uncertainty distributions for the surface and ocean temperatures under the ECPs. In our simulations of future solid ice discharge, we combined climate and ice-model uncertainty by forcing each of the 81 initial states from the perturbed-physics ensemble with the 33rd, 50th and 66th percentile of the temperature uncertainty distributions. Our results are thus based on a set of 972 simulations. To separate the effect of snowfall on solid ice discharge from the effects of surface warming and enhanced sub-shelf melting, the whole set of simulations was performed for the cases of surface warming only, surface and ocean warming, and surface and ocean

warming including snowfall increase. The dynamic response of the perturbed-physics ensemble to the climate scenarios is further discussed in ref. 24.

**Sub-shelf melting.** To simulate the main overturning circulation in the sub-ice shelf cavities, which greatly influences the local distribution of basal melting and refreezing, an ocean box model<sup>17</sup> was used. The ocean box model was initialized with recently observed ocean temperatures and salinities<sup>17</sup> near the Ross, Filchner-Ronne and Amery Ice Shelves as well as the shelf attached to Pine Island Glacier, from which we subtracted anomalies of the observational period to 1850 (the first year of the simulations). Sub-shelf melting was then computed from the ocean temperature and salinity provided by the ocean box model as well as changes in ice thickness and thus pressure melting temperature at the underside of the ice shelves. This approach enables the model to capture the wide spread of observed melt rates underneath Antarctic ice shelves<sup>12</sup>. Modelled basal melt rates peak near the grounding line, as suggested by observations<sup>30</sup>.

**Blowing snow sublimation and redistribution.** Blowing snow sublimation and redistribution might affect the results because it mainly occurs along the coastal margins of Antarctica<sup>31</sup>, where the impact of enhanced snowfall on the ice dynamics is greatest. The increase of relative humidity in the lower atmosphere due to blowing snow leads to an increase in snowfall, especially in the coastal areas where the air is close to saturation<sup>31</sup>. This suggests that the impact on the ice dynamics presented here would be enhanced by blowing snow. However, this is likely to be a higher-order effect because the temporal trends in coastal blowing snow accumulation will be negligible compared to the overall increase in snowfall.

28. van Vuuren, D. *et al.* The representative concentration pathways: an overview. *Clim. Change* **109**, 5–31 (2011).
29. Taylor, K., Stouffer, R. & Meehl, G. An overview of CMIP5 and the experiment design. *Bull. Am. Meteorol. Soc.* **93**, 485–498 (2012).
30. Walker, R. T., Dupont, T. K., Parizek, B. R. & Alley, R. B. Effects of basal-melting distribution on the retreat of ice-shelf grounding lines. *Geophys. Res. Lett.* **35**, L17503, <http://dx.doi.org/10.1029/2008GL034947> (2008).
31. Lenaerts, J. T. M. & van den Broeke, M. R. Modeling drifting snow in Antarctica with a regional climate model: 2. Results. *J. Geophys. Res.* **117**, D05109, <http://dx.doi.org/10.1029/2010JD015419> (2012).